Letters in Applied NanoBioScience
Open-Access Journal (ISSN: 2284-6808)

Article
Volume 12, Issue 3, 2023, 61
https://doi.org/10.33263/LIANBS123.061

Green Synthesis of *Tecoma stans* Flower and Leaf Extracts: Characterization and Anti-Proliferative Activity in Colorectal Cancer Cell Lines

Kousalya Lavudi [1], GVS Harika [2], Anand Thirunavukarasou [3,4], Gulothungan Govindarajan [5], Srinivas Patnaik [1], Narasimha Golla [6], Venkata Subbaiah Kotakadi [7], Josthna Penchalaneni [2,*]

1 Department of Biotechnology, KIIT University, Bhubaneswar - 751024, Odisha, India; kowsi.bio@gmail.com (K.L.); srinivas.patnaik@kiitbiotech.ac.in (S.P.);
2 Sri Padmavathi Mahila Visvavidyalayam, Tirupathi - 517502, Andhrapradesh, India; harika.biotech@gmail.com (G.V.S.H.); penchalajyo@yahoo.co.in (J.P.);
3 B-Aatral Biosciences Pvt. Ltd, Bengaluru - 560091, Karnataka, India; anandarasou28@gmail.com (A.T.);
4 Saveetha School of Engineering, Saveetha Institute of Medical and Technical Sciences, Chennai - 600077, Tamilnadu, India; anandarasou28@gmail.com (A.T.);
5 Vel Tech Rangarajan Dr. Sagunthala R& D Institute of Science and Technology. Chennai - 600062, Tamilnadu, India; g.gulothungan@gmail.com (G.G.);
6 Department of Virology, Sri Venkateswara University, Tirupathi - 517502, Andhrapradesh, India; dr.g.narasimha@gmail.com (N.G.);
7 DST Purse Centre, Sri Venkateswara University, Tirupathi - 517502, Andhrapradesh, India; kotakadi72@gmail.com (V.S.K.);
* Correspondence: penchalajyo@yahoo.co.in (J.P.);

Scopus Author ID 14035779800
Received: 25.02.2022; Accepted: 27.03.2022; Published: 15.04.2022

Abstract: Since times immemorial, many plant species have been utilized to cure severe diseases. A wide range of diversification has been observed in various medicinal plants, which are indeed able to cure several deadly diseases. The presence of secondary metabolites is a high priority for their medicinal characteristics. This study focused on *T. stans* (Yellow bells), a shrub that grows profoundly in tropical and sub-tropical regions. Although many studies have been done on the medicinal value of this plant, not much has been done on cancer treatment and nanomedicine. Green synthesized silver nanoparticles are an eco-friendly approach to delivering the drug to the target size. Nano appearance is an add-on advantage of these compounds. Hence, it is emerging in medicine. Colorectal cancer is the fourth deadliest one globally. Hence the synthesized silver nanoparticles of *T. stans* flower and leaf extracts showed cytotoxically and wound healing properties on colorectal cancer cell lines (HCT 116 and SW 480). Synthesis of silver nanoparticles confirmation is done by Ultra Violet Visible spectrophotometry and Particle size analyzer. All the results showcase the beneficial effects of silver nanoparticles synthesized plant extracts and may be used as a novel medicine in the field of chemotherapy.

Keywords: silver nanoparticles; *Tecoma stans*; flower and leaf extracts; wound healing property.

1. Introduction

In nature, plant species play a magnificent role in treating several disorders caused by bacteria, viruses, nematodes, and fungal species [1–3]. Various cultures and demographics use their native plant species, which possess several bioactive compounds, to cure deadly diseases [4–6]. Secondary metabolites are the primary sources of bioactivity in most plant species [7–

9]. *Tecoma stans*, called yellow bells, are a popular ornamental plant belonging to the family Bignoniaceae and are popularly distributed in tropical and sub-tropical regions [10,11]. *T. stans* is a unisexual, deciduous shrub with 5.6 - 7 m in height. In Costantino *et al*. (2003) study, flower and leaf infusions can be taken orally for diabetes and stomach pains [11]. A strong leaf and root decoction can be taken orally as a diuretic to treat syphilis or intestinal worms [12]. *T. stans* is known to have various medicinal and therapeutic properties. *T. stans* leaves contain potent anti-inflammatory and analgesic activities that have been evaluated as antibacterial agents against some human bacterial strains [13,14]. In addition, flowers and barks are traditionally used to treat various cancers [15]. Amongst nine plants studied, *T. stans* were found to give the best inhibition zones against fungal activity [16].

Several reports have identified secondary metabolites like sterols, phenols, tannins, phytosterols, and many more. [17]. studies have shown the wound healing nature of *T. stans* methanolic extracts [18]. Moreover, usage of several solvent extractions has shown significant antibacterial and antioxidant activities [19]. The taxonomic classification of the plant is as follows: Plantae (Kingdom), Angiosperms (Clade), Lamiales (Order), Bignoniaceae (Family), Tecoma (Genus), and stans (Species). Nanotechnology is currently an emerging field with medical, electronic, and structural designs [20]. The particles' tiny size reflects their name and gives a maximum benefit to their existence. The flexibility in their size helps these particles to enter minute blood vessels to deliver the drug and hit the target at the point [21]. This feature made nanoparticles form a major platform in nanomedicine and drug delivery [22].

Colorectal cancer is the third emerging cancer in fatality and the fourth most dominating cancer globally in mortality rate. Around 25% of cases exhibit recurrence annually [23]. In recent years, recurrence of the disease has become a major concern [24]. This led to the development of tumors most aggressively. Standard drugs such as oxaliplatin control the growth of tumors at the initial stages, but the tumor becomes resistant after some time [25]. Hence, using bioactive compounds with nanoparticles increases the treatment efficiency. Although *T. stans* plant parts exhibit diverse medicinal properties in treating various diseases, silver nanoparticle (AgNP) synthesis using methanolic extracts in cancer treatment was not evaluated scientifically. Preliminary studies in this aspect could create an open platform in clinical research and combinational therapy.

In our current study, we have used *T. stans* leaf and flower extracts to evaluate their role in anti-proliferation and wound healing properties. AgNPs were synthesized using methanolic extracts, and characterization studies were performed using Ultra Violet Visible (UV-Vis) spectrophotometry. The synthesized AgNPs were further studied to determine their size and charge using a particle size analyzer and zeta potential. Functional group characterization was performed using Fourier Transform Infra-Red (FT-IR) study. Antioxidant properties were examined in comparison between both crude extracts and AgNPs. The antimicrobial activity was studied against both gram-positive and gram-negative bacteria. Anti-proliferative activity was studied using HCT-116 and SW 620 cell lines. HEK 293 was used as a control. Finally, wound healing properties were studied using different concentrations of AgNPs.

2. Materials and Methods

2.1. Collection of leaf and flower extracts.

The leaves and flowers of *T. stans* (commonly called yellow bells) were collected from the trees growing around the Sri Padmavati Mahila University (SPMVV), Tirupati, Chittoor district, Andhra Pradesh, India. The plant was identified and authorized by the Professor. B. Nagaraj, Taxonomist, Department of Botany, Sri Venkateswara University, Tirupati, Andhra Pradesh, India. The collected plant parts were rinsed with double distilled water to remove the dirt present on the surface and then chopped into small pieces. The leaves and flowers were allowed to shade dry for about 7-10 days.

2.2. Preparation of plant extracts.

The nanoparticles were synthesized using plant extract, which reduces the generation of hazardous substances. *T. stans* leaf and flower extracts were taken and shade dried for about one week. The shade dried leaves and flowers were ground separately with the help of a blender, and the coarse powder was collected in zip lock covers for future use. 7.5 gms of powder was weighed, and Soxhlet with 250ml of 80% methanol was used as a solvent system for extraction by using a Soxhlet extractor for 7 cycles up to 8 hours at 64°C until the solvent in the siphon tube became colorless. A Rotary Flash evaporator was used to remove the solvents from the plant sample by evaporation at 64º C for 1 hr. The solvent (methanol) was separated and collected in the tube and can be reused. The crude extract was collected in a Petri dish and allowed to air dry. The collected extract was stored in a scintillation flask and can be used for analysis.

2.3. Preparation of AgNPs.

The crude sample was prepared with a concentration of 10mg/ml by adding distilled water. 2 ml of the crude sample was taken, and the volume was made up to 5 ml by adding distilled water. 10 ml of 1 mM Silver Nitrate ($AgNO_3$) solution was added to the extract and kept in a water bath for reduction reaction at 70 - 80ºC for about 30 minutes. The color change observed indicates the AgNP's were synthesized, and a peak was observed.

2.4. Phytochemical analysis for leaf extracts.

Phytochemicals in leaf extracts were identified using several different approaches. 1. Test for alkaloids, (a) Mayer's test (to a few ml of filtrate, a few drops of Mayer's reagent were added along the sides of the test tube), and (b) Wagner's test (To 1ml of plant extract, few drops of Wagner's reagent were added along the sides of the test tube). 2. Test for Tannins, (a) Ferric Chloride Test (0.5g of the extract was boiled in 10ml of distilled water and filtered. 5ml of the filtrate was taken in a test tube and a few drops of 0.1% $FeCl_3$ were added). 3. Test for Saponins, (a) Froth Test (About 0.2 g of the extract was shaken with 5 ml of distilled water and then heated to boil. Frothing shows the presence of saponins). 4. Test for Phenols, (a) $FeCl_3$ test (50ml of the extract is dissolved in 5ml of distilled water, and a few drops of neutral $FeCl_3$ were added). 5. Test for steroids, (a) Lieberman Burchard's test (20mg of the extract was treated with 2.5ml of acetic anhydrite and 2.5ml of chloroform, then H_2SO_4 was added slowly). 6. Test for terpenoids, (a) Salkowski's test (Extracts were treated with chloroform and filtered, and the filtrates were treated with a few drops of a concentrated solution of H_2SO_4). 7. Test for

Flavonoids, (a) Lead acetate test (To 1ml of extract 1ml of 10% lead acetate was added) and (b) Alkaline reagent test (Extracts were treated with few drops of NaOH solution and formation of intense yellow color, which become colorless on the addition of dilute acid). 8. Test for glycosides, (a) Cardiac glycosides (To 5 ml of extract 2ml of glacial acetic acid, a few drops of $FeCl_3$ and 1ml of H_2SO_4 were added). The phytochemical analysis of *T. stans* flower extracts has already been reported in the literature [13,26,27], and it has negligible bioactive components compared to T. stans leaf extracts.

2.5. Antimicrobial activity.

Bacterial strains used for antimicrobial activity are *Escherichia coli, Bacillus subtilis, Klebsiella Pneumoniae,* and *Staphylococcus* obtained from the microbiology lab in our department. These strains are activated at 37º C for 24hour. Antibacterial activity was assayed by the agar well plate method and used to detect the antibacterial activities of synthesized nanoparticles. After solidifying the media with bacterial culture, the wells were made by using a sterile cork borer. Wells of 6 mm size were made into the agar set plate containing the bacterial culture, and the lower portion was sealed with a little molten agar media. Different concentrations of (10, 20, 30, and 40 µg/ml) were placed into each well. The crude extract was placed in the middle of the Petri plate. The culture plates were incubated at 37ºC for 18-24 hrs, and antibacterial activity was evaluated by measuring the radius of the zone of inhibition. The zone of inhibition was compared with that of standard antibiotic (levofloxacin) plates.

2.6. Antioxidant assay.

Different concentrations of synthesized nanoparticles (100,200,300,400,500µl) were taken in different vials and then made up to 1 ml with methanol. Ascorbic acid was taken as standard, and DPPH was used as control. Add 1 ml of 0.1 mM DPPH solution to the test tubes. The test tubes were shaken and incubated for 30min in darkness. The absorbance of the samples was measured against blank (methanol) at 517nm using UV-Spectrophotometer. DPPH scavenging activity was expressed as the % inhibition of the free radical DPPH.

% of inhibition = (A control –A sample / A control) X 100
A sample =absorbance of the sample
A control = absorbance of DPPH

2.7. MTT assay.

When the cultured cells reached 80% confluency, cells were trypsinized using 0.25% trypsin, followed by counting and respective seeding (1x105) in a 96 well plate and kept in an incubator containing 5% of CO_2, at 37ºC for 24hrs. C1 - Medium control, C2 – Cell control, C3 - Drug control were used. S1, S2, S3, S4, S5, S6 were considered standards. After 24 hrs, the cells were treated at various leaf and flower AgNP extracts concentrations respectively (25, 50, 100, 200, 300, and 400µg/ml). After 24 hrs, 10µl of MTT solution was added to each well, including control, and incubated for 2-4 hrs in the incubator. After the incubation, 100µl of solubilization solution was added and stirred gently on the gyratory stirrer to ensure crystal dissolution. Absorbance was taken on an ELISA reader at 570nm with a reference wavelength higher than 650 nm. The graph was plotted by taking concentration on X-axis and OD values on Y-axis.

2.8. Wound healing assay.

1*106 cells were seeded in a 6 well plate, and the cells were incubated in a CO2 incubator for 24 hrs. Once the cells reached 90% confluency, a scratch was given using a 10 µl sterile tip in a straight line. By taking the IC50 value as a reference, the cells were treated with two different concentrations. At 0 hours, an image was captured using an inverted microscope, and ZEN software was used for analysis. To check the efficiency of migration, another image was captured after 24 treatments. The migration distance was calculated using Image J.

3. Results and Discussion

3.1. Green synthesis of silver nanoparticles.

Colorless plant extracts prepared from the powdered leaf and flowers of *T. stans* contain several molecules that can reduce silver ions to AgNPs by changing the color to dark green after heating at 80ºC for 20 minutes. Figure 1A represents the synthesis of AgNPs using leaf extracts, and Figure 1B represents the synthesis of AgNPs using flower extracts of *T. stans*. The color change confirms that it was due to the reduction of Ag+, which indicates the formation of AgNPs.

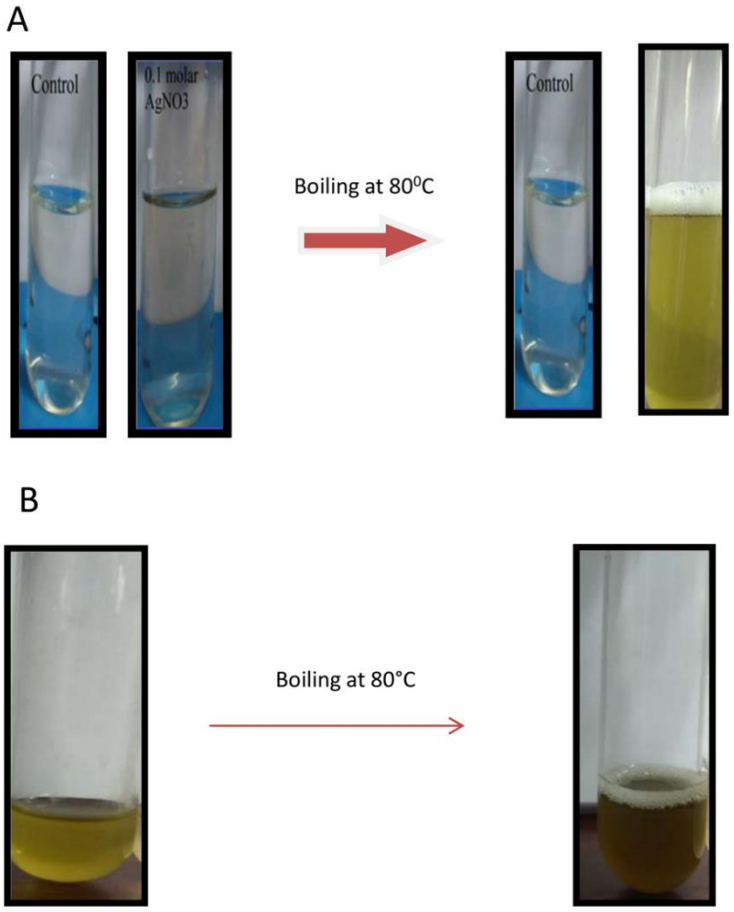

Figure 1. The figure confirms the color change in *T. stans* flower extracts. Color change indicates the synthesis of AgNPs.

3.2. UV-Visible spectrophotometry.

The optical property of AgNPs can be determined by using UV-Vis spectrophotometry. A surface plasmon resonance spectrum shows a characteristic peak at a range of 300 nm - 700

nm, confirming the synthesis of AgNPS. *T. stans* flower shows peak absorbance at 436 nm (Figure 2A), and the *T. stans* leaf shows maximum absorbance at 446 nm (Figure 2B).

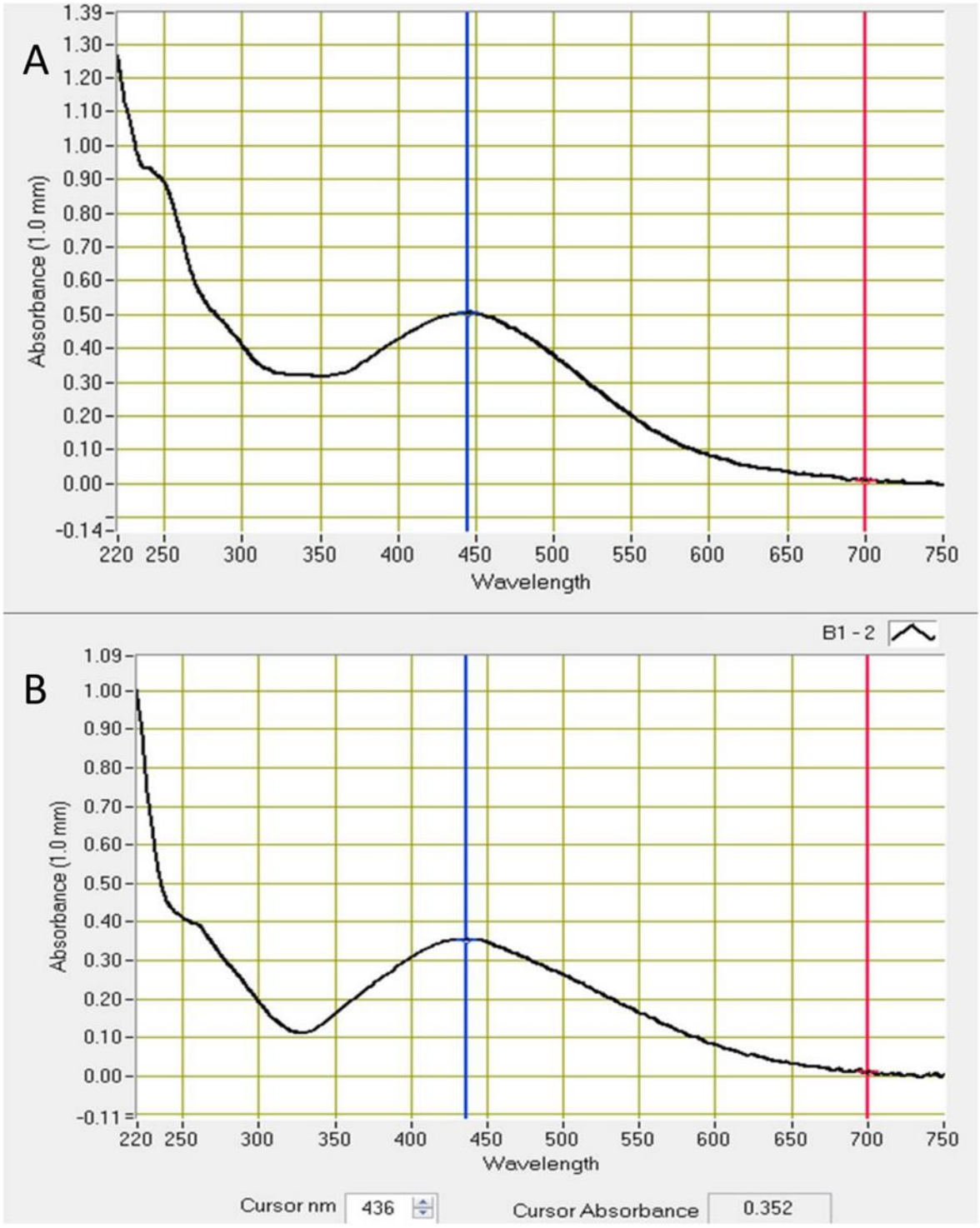

Figure 2. AgNP absorption spectra of (**A**) *Tecoma stans* flower; (**B**) *Tecoma stans* leaf extracts using 0.1M $AgNO_3$.

3.3. Particle size determination.

A particle size analyzer is a scientific tool that measures, depicts, and reports the particle size distribution for a synthesized nanoparticle. The particle size of the AgNPs obtained is detected by intensity and laser diffraction, which are polydispersed mixture solutions presented in Figure 3. A particle size analyzer was used to study the method. The size of synthesized *T.*

stans flower AgNPs ranged from 30-50nm (Figure 3B), and the size of leaf extracts ranged from 60-111.7 nm (Figure 3A). Here, we observed a larger particle size for *T. stans* leaves than flowers. AgNPs' extremely small dimensions (*T. stans* flowers) make them beneficial for antibacterial effects and attacking intracellular microorganisms. Small-sized silver nanoparticles (20-60 nm) generally have excellent antibacterial activity [28,29]. Because these particles only work when they contact bacterial cell walls, there are several ways to encourage nanoparticle-bacterial interaction [30]. Nanoparticles can penetrate microbial membranes, interfere with metabolic processes, and cause membrane structure and function after contact. Once within cells, nanoparticles interact with bacteria's cellular machinery to block enzymes, deactivate proteins, cause oxidative stress and electrolyte imbalance, and alter gene expression levels.

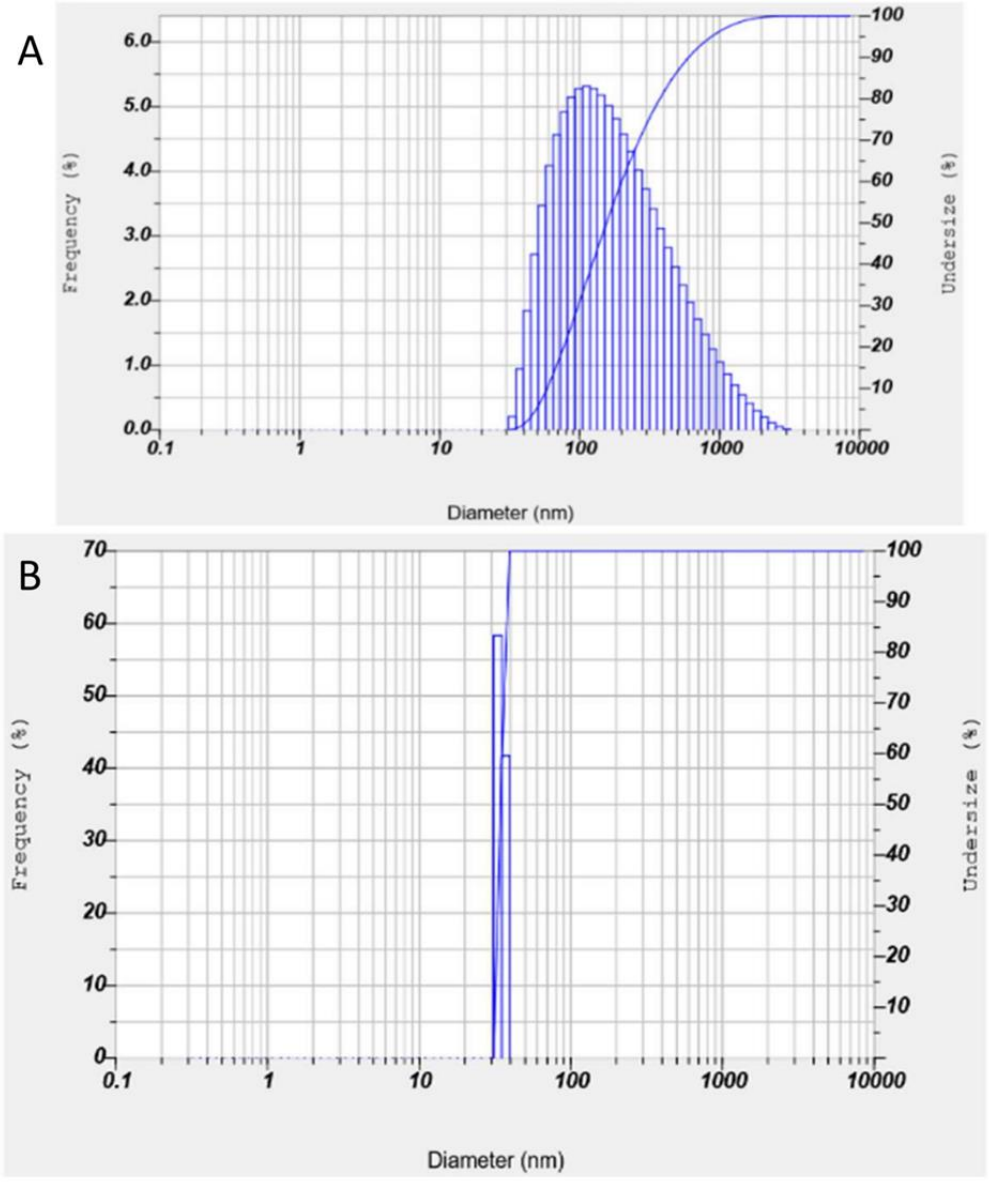

Figure 3. The particle size of both flower and leaf extracts. (**A**) Particle determination of leaf (111.7nm) (**B**) Particle size determination of flower (34.7nm).

3.4. Zeta potential analysis.

The electrostatic repulsive force between the nanoparticles depends on the charge present on the particle's surface. The negative zeta potential value confirms the repulsion

among the particles, thereby increasing the formulation's stability and preventing the nanoparticles from agglomeration in the medium, leading to long-term stability. The zeta potential of the AgNPs of *T. stans* leaf extract was found to be -17.1mV (Figure 4A), and flower extract was found to be –31.5mV (Figure 4B). It was concluded that the AgNPs synthesized with *T. stans* leaf extract were moderately stable, and AgNPs of flower extracts were highly stable.

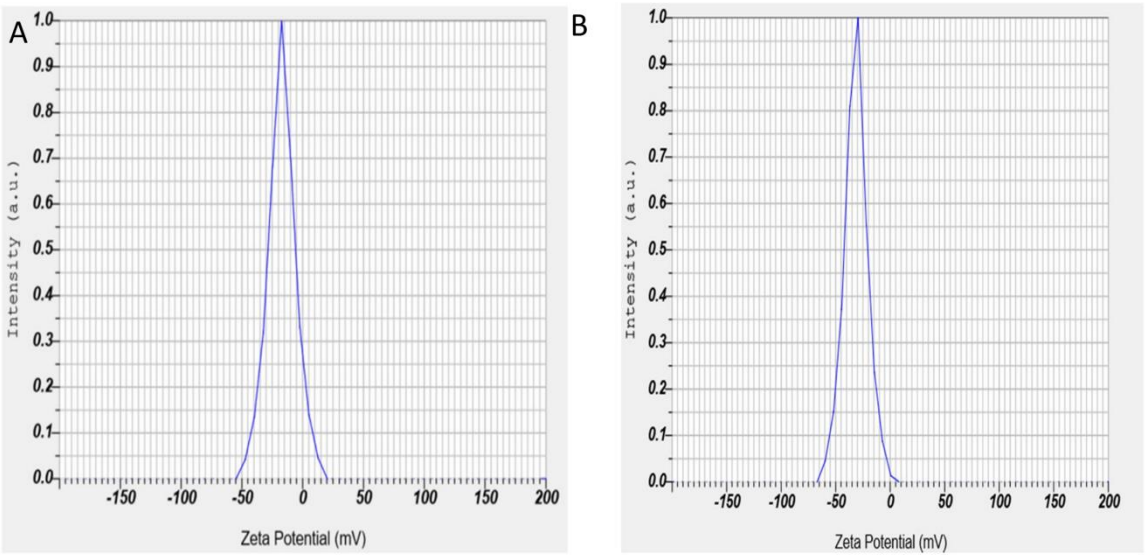

Figure 4. (**A**) Zeta potential of the AgNPs of *Tecoma stans* leaf extracts (-17.1mV); (**B**) Zeta potential of flower extracts (-31.5mV).

3.5. Phytochemical screening of leaf extracts.

Phytochemical analysis was performed using standard protocols [31]. These tests confirmed the presence of secondary metabolites such as Alkaloids, Flavonoids, Glycosides, Phenols, Tannins, Steroids, Terpenoids, and Saponins in leaf extracts of *T. stans* (Supplementary Table 1). In addition, the confirmation of secondary metabolites was observed by respective color changes (Figure 5).

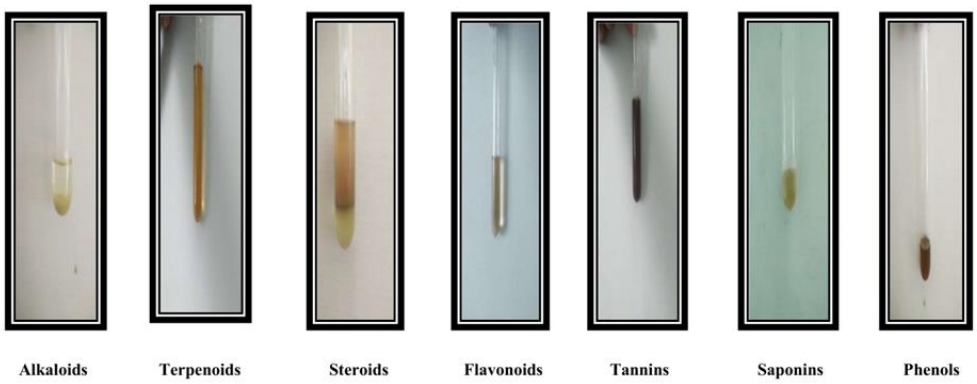

Figure 5. Shows the color formation of respective secondary metabolites.

3.6. FTIR analysis.

FTIR Pattern of the synthesized nanoparticles was studied. It ranges from 500-3500 cm^{-1}. Figures 6a and 6b show functional groups of crude leaf extract and synthesized AgNPs of *T. stans*. FTIR spectrum of crude leaf extract showed significant peaks at 2852.16, 1383.45, 667.87,1019.50, 3399.88, 1743.38, which corresponds to the presence of alkanes, alkenes,

alkyl halides, alcohols, ketones, esters, and amides. The *T. stans* leaf AgNPs showed significant peaks at 2854.58, 2923.81, 668.20, 1089.31, 1270.70, 1319.29, 1626.01, 1741.96, 2854.58, 2923.91,3420.81, 1270.70,1626.02, 779.91, which corresponds to the presence of alkanes, alkenes, alkynes, alkyl halides, alcohols, ethers, aldehydes, ketones, carboxylic acids, esters, amides and aromatic compounds (Supplementary Table 2). Figures 6c and 6d represent the FT-IR peaks of *T. stans* crude and AgNPs of flower extracts. *T. stans* crude flower and AgNPs possess functional compounds such as alkyl halides, alkanes, alkyls, amides, carboxylic acids, and ketones (Supplementary Table 3). Figure 6a, 6b, 6c, and 6d show FTIR spectra of both crude and AgNP synthesized particles of both *T. stans* leaf and flower. Supplementary Table 2 and Supplementary Table 3 show the functional compounds present in leaf and flower crude and AgNP extracts.

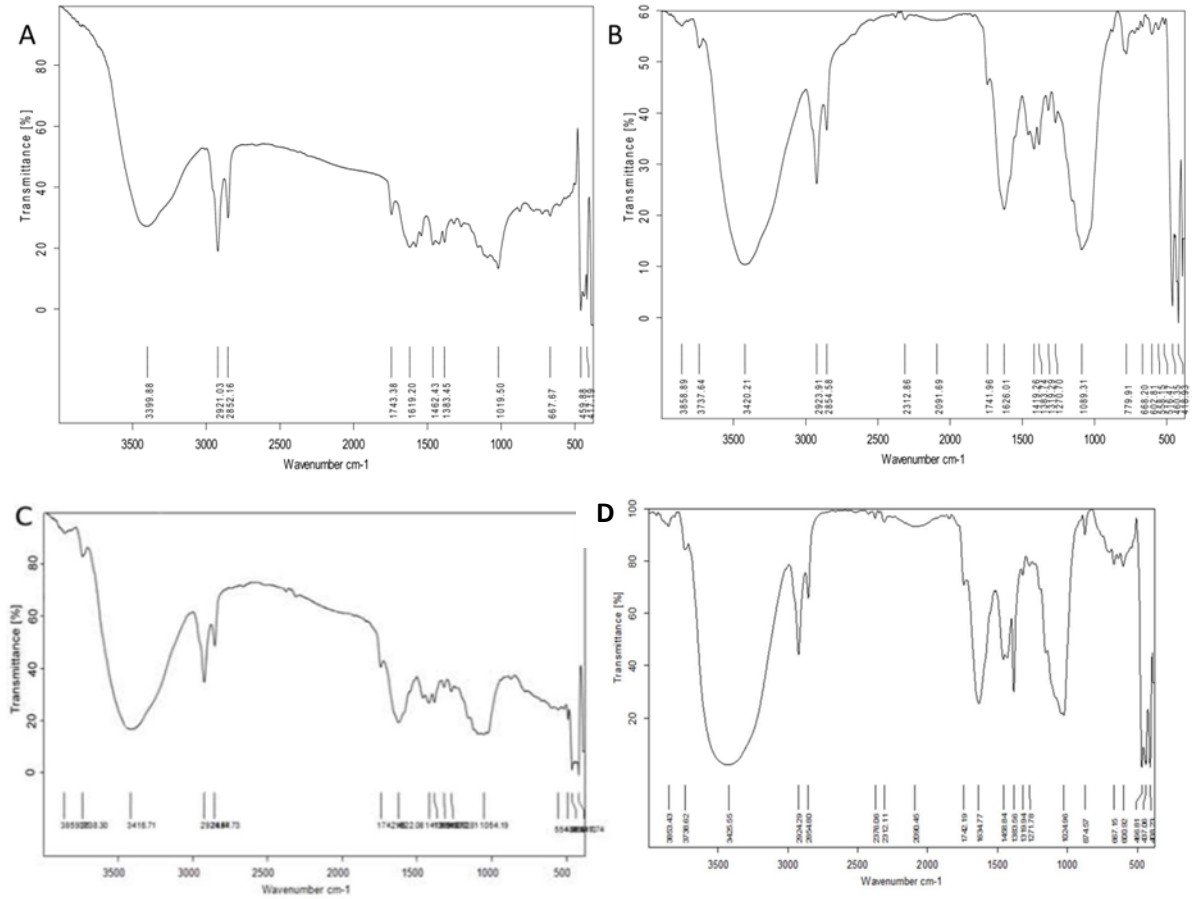

Figure 6. A. Represents the FTIR spectral study of *Tecoma stans* leaf Crude extract. B. Represents the FTIR spectral study of *Tecoma stans* leaf AgNPs. C. Represents the FTIR spectral study of Tecoma stans flowers crude extract. D. Represents the FTIR spectral study of *Tecoma sta*ns flower AgNPs.

3.7. Antimicrobial activity.

The antibacterial activity of the sample was identified by measuring the zone of inhibition. The size of the zone of inhibition is a measure of the compound's effectiveness. The antimicrobial activity of *T. stans* leaf extract was studied at different concentrations (10, 20, 30, 40µg/ml) against *Escherichia coli, Bacillus subtilis, Klebsiella pneumoniae, Staphylococcus aureus.* It was confirmed that the antibiotic (levofloxacin) and plant extracts had shown the inhibition zones. The plant extract showed antibacterial activity at different ranges. The maximum zone of inhibition was observed in *E. coli*, followed by *K. pneumoniae*,

and *S. aureus*. The zone of inhibition was measured and calculated. (Supplementary Table 4). The leaf AgNP extracts have shown a better inhibition zone than the flower AgNP extracts of *T. stans* (Figure 7A-D).

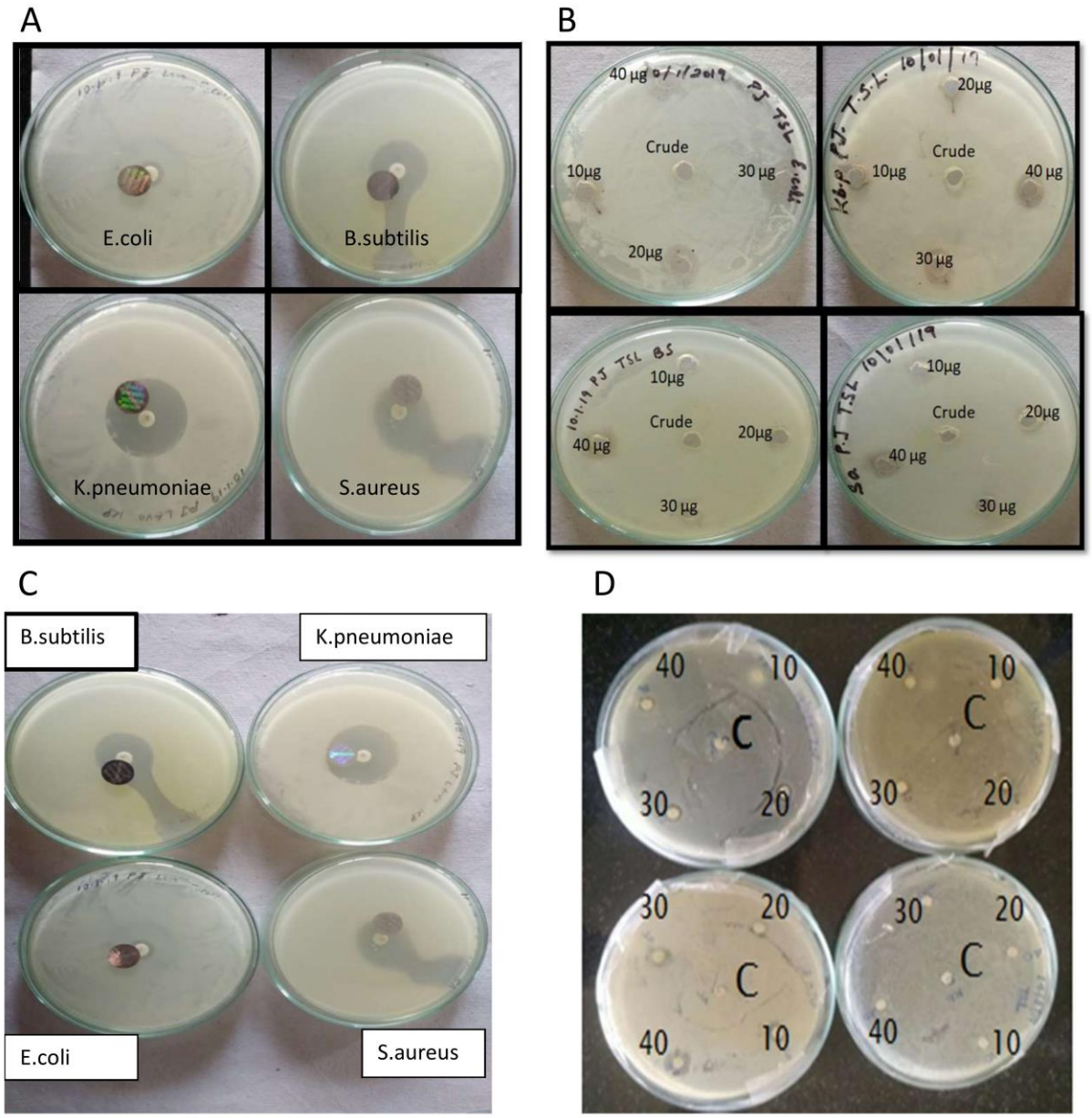

Figure 7. **A** and **C** represent the levofloxacin controls. **B** and **D** represent *T. stans* leaf and flower AgNPs.

3.8. Free radical scavenging activity.

Antioxidant activity of silver nanoparticles synthesized from *T. stans* leaf extract was studied by DPPH free radical scavenging assay. This method is dependent on reducing DPPH radical to the ion-radical form DPPH-H in the presence of a hydrogen donating antioxidant. The radical scavenging activity (RSA) values of AgNPs and crude extract values were represented in Supplementary Table 5. The RSA of AgNPs was increased with an increase in the concentration, and the highest RSA was observed at the highest test concentration of 500µg/ml used in this assay was found to be 70.694% (Figure 8).

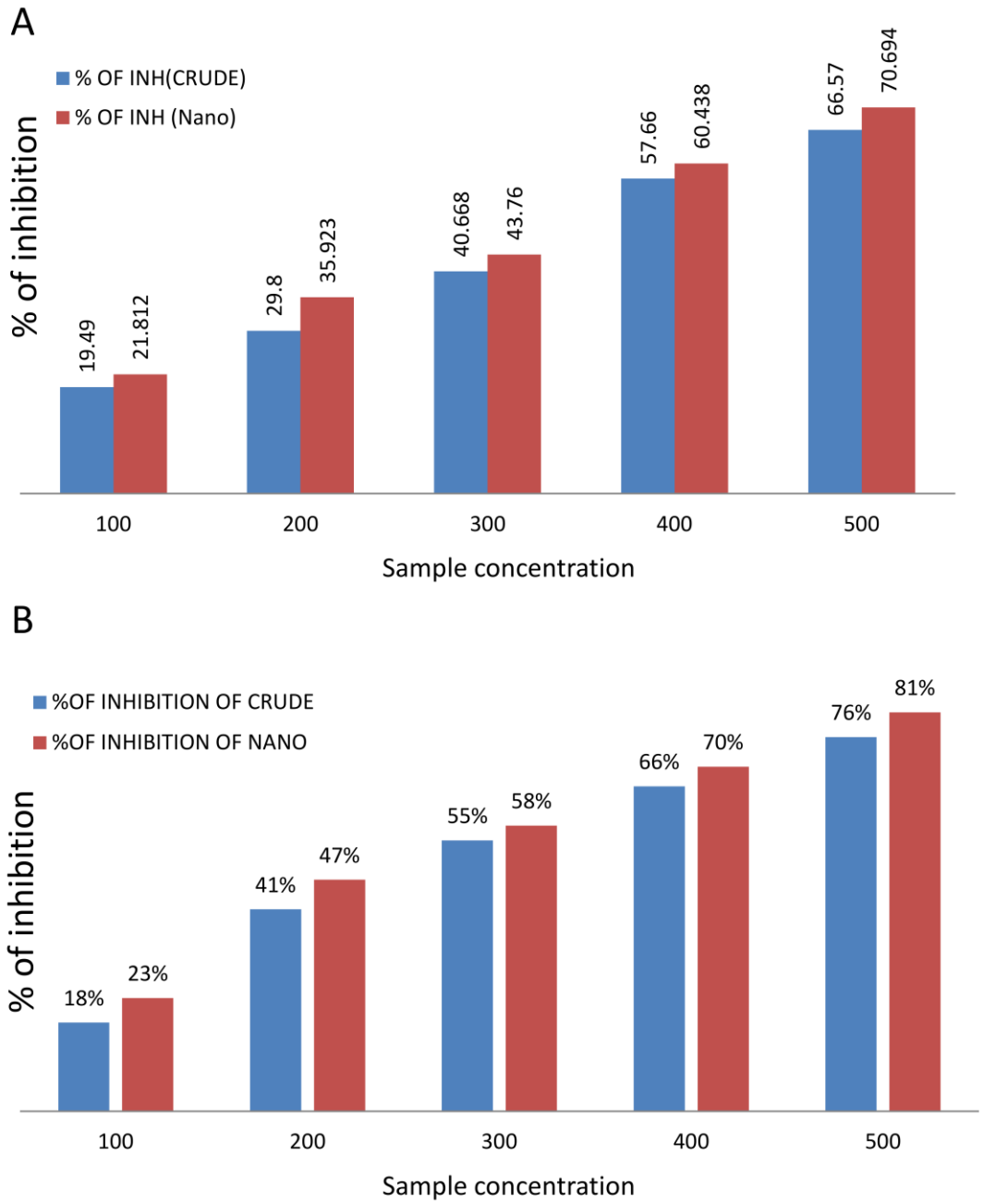

Figure 8. A represents the free radical inhibition of *T. stans* leaf (crude vs. AgNPs), and B represents the free radical inhibition of *T. stans* flower (crude vs. AgNPs).

3.9. MTT assay.

Methanolic extract of *T. stans* was applied to the HCT116 cell line. The IC50 doses were measured and incubated at 37ºC in darkness. HCT 116 cells with DMEM were replaced every 3 days and incubated for 24hr. The number and diameter of colonies within each cell were counted each day under the microscope, and the images were captured for the representative fields. Figure 9 (A, B, C, and D) are the microscopic observations of the HCT 116 cell line at different test sample concentrations. Supplementary Figure S1 shows the anti-proliferative activity against the *T. stans* AgNP flower extracts at different concentrations. In addition, Supplementary Figure S2 presents the graphical representation of anti-proliferative activity against colorectal cancer cell lines. HEK 293 is used as a control.

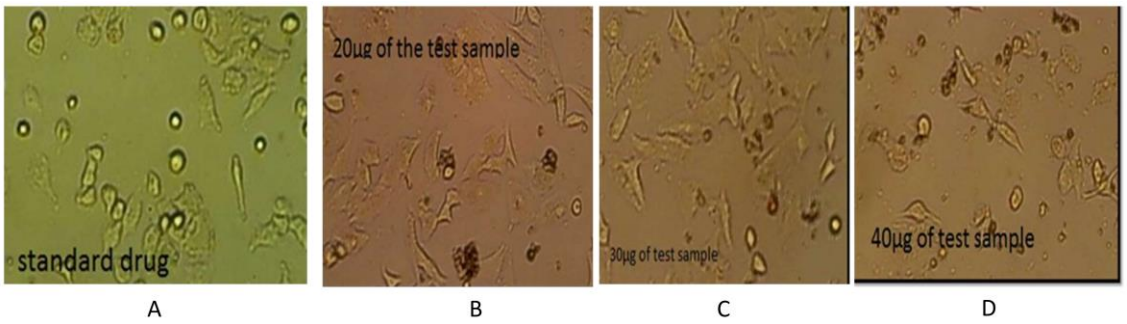

Figure 9. **A**, **B**, **C,** and **D** represents the microscopic observations of the HCT 116 cell line at different test sample concentrations.

3.10. Wound healing assay.

Migration capacity has been calculated by performing the wound healing assay. At higher concentrations, migration capacity has been reduced, which shows that *T. stans* AgNPs might potentially reduce the migration of CRC tumor cells at defined concentrations. Figures 10 A and B represent the wound healing activity of the *T. stans* flower AgNPs extract against SW480 cell line and *T. stans* leaf in HCT 116 cell lines, and 10C represents the pictorial representation of the area covered after 24 hours.

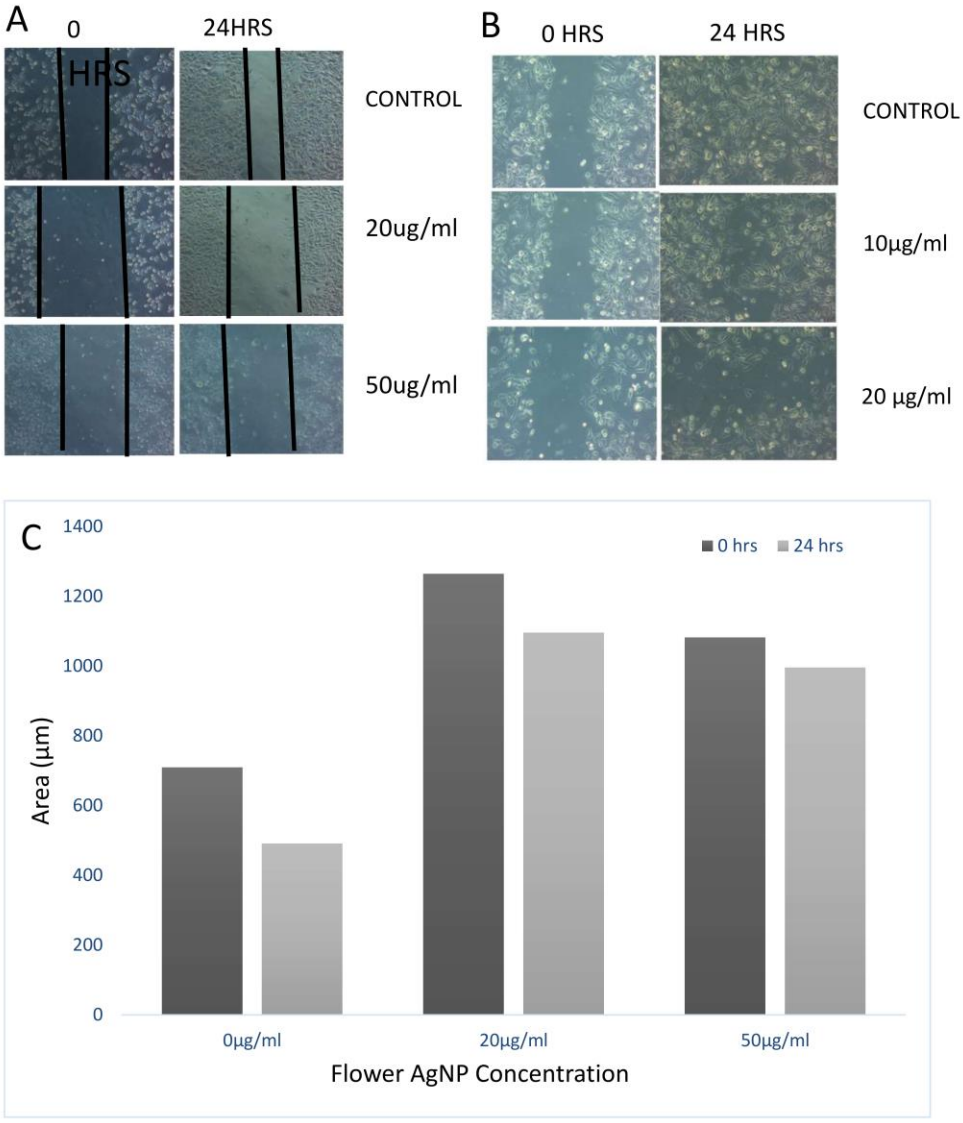

Figure 10. **A** and **B** – wound healing property of *T. stans* flower and leaf extracts. Figure C represents a graphical representation of area covered after 24 hours. Distance is calculated using Image J.

4. Conclusions

The biological synthesis of silver nanoparticles using *T. stans* leaf and flower extracts provides an environmentally friendly, simple, and efficient route for synthesizing benign nanoparticles. Phytochemical screening studies of leaf extracts show a high concentration of bioactive compounds such as terpenoids, flavonoids, tannins, alkaloids, and saponins. The leaf nanoparticles contain functional groups such as amines, alcohols, ketones, aldehydes, etc., which were found from the characterization using a UV-visible spectrophotometer, zeta potential, and particle size analyzer. FTIR analysis for flower extracts was performed and confirmed the presence of different functional groups. The data concludes that more functional compounds are present in *T. stans* flower AgNPs extract than in the crude sample.

DPPH radical scavenging activity of the synthesized AgNPs increased by increasing the concentration in *T. stans* leaf extracts. The free radical scavenging activity is more in AgNPs extract when compared with the crude extract of *T. stans* flower. The synthesized leaf AgNPs possesses antibacterial activity against different pathogenic species such as *E. coli, B. subtils, S. aureus, K. pnuemoniae*. The antimicrobial activity of silver nanoparticles of *T. stans* flower, when compared with the standard drug, shows less antimicrobial activity. Cytotoxicity assay reveals that the leaf extracts possess anti-proliferative activity, and IC50 value was determined in both leaf and flower extracts. The wound-healing assay was performed to check the healing activity of the AgNPs extract of *T. stans* flower and leaf. With an increase in its concentration, we can see the number of cells decreasing within the scratch that was made. Hence it was proven that it has wound healing properties. *T. stans* Leaf and flower extracts have potential applications in the field of medicine. Our *in vitro* studies showed the anti-proliferative activity against colorectal cancer cell lines, and *in vivo* studies are required to know the major potential.

Funding

This research received no external funding.

Acknowledgments

Declared none.

Conflicts of Interest

The authors declare no conflict of interest.

References

1. Balaraman, R. *et al*. A Review on the Biological Effects of some Natural Products. *Journal of Natural Remedies* 2020, 117-127, http://dx.doi.org/10.18311/jnr/2020/25581.
2. Zhang, H.; Li, J.; Saravanan, K.M.; Wu, H.; Wang, Z.; Wu, D.; Wei, Y.; Lu, Z.; Chen, Y.H.; Wan, X.; Pan, Y. An Integrated Deep Learning and Molecular Dynamics Simulation-Based Screening Pipeline Identifies Inhibitors of a New Cancer Drug Target TIPE2. *Front. Pharmacol.* **2021**, *12*, 772296, https://doi.org/10.3389/fphar.2021.772296.
3. Yuan, M.; Ngou, B.P.M.; Ding, P.; Xin, X.-F. PTI-ETI crosstalk: an integrative view of plant immunity. *Curr. Opin. Plant Biol.* **2021**, *62*, 102030, https://doi.org/10.1016/j.pbi.2021.102030.
4. Manzoor, M.; Singh, J.; Gani, A.; Noor, N. Valorization of natural colors as health-promoting bioactive compounds: Phytochemical profile, extraction techniques, and pharmacological perspectives. *Food Chem.* **2021**, *362*, 130141, https://doi.org/10.1016/j.foodchem.2021.130141.
5. Roy, A.; Datta, S.; Bhatia, K.S.; Bhumika; Jha, P.; Prasad, R. Role of plant derived bioactive compounds

against cancer. *South African J. Bot.* **2021**, https://doi.org/10.1016/j.sajb.2021.10.015.
6. Nguyen, P.; Doan, P.; Rimpilainen, T.; Konda Mani, S.; Murugesan, A.; Yli-Harja, O.; Candeias, N.R.; Kandhavelu, M. Synthesis and Preclinical Validation of Novel Indole Derivatives as a GPR17 Agonist for Glioblastoma Treatment. *J. Med. Chem.* **2021**, *64*, 10908–10918, https://doi.org/10.1021/acs.jmedchem.1c00277.
7. Chiocchio, I.; Mandrone, M.; Tomasi, P.; Marincich, L.; Poli, F. Plant Secondary Metabolites: An Opportunity for Circular Economy. *Molecules* **2021**, *26*, 495, https://doi.org/10.3390/molecules26020495.
8. Ramakrishna, W.; Kumari, A.; Rahman, N.; Mandave, P. Anticancer Activities of Plant Secondary Metabolites: Rice Callus Suspension Culture as a New Paradigm. *Rice Sci.* **2021**, *28*, 13–30, https://doi.org/10.1016/j.rsci.2020.11.004.
9. Jacoby, R.P.; Koprivova, A.; Kopriva, S. Pinpointing secondary metabolites that shape the composition and function of the plant microbiome. *J. Exp. Bot.* **2021**, *72*, 57–69, https://doi.org/10.1093/jxb/eraa424.
10. Vaou, N.; Stavropoulou, E.; Voidarou, C.; Tsigalou, C.; Bezirtzoglou, E. Towards Advances in Medicinal Plant Antimicrobial Activity: A Review Study on Challenges and Future Perspectives. *Microorganisms* **2021**, *9*, 2041, https://doi.org/10.3390/microorganisms9102041.
11. Aguilar-Santamaría, L.; Ramírez, G.; Nicasio, P.; Alegría-Reyes, C.; Herrera-Arellano, A. Antidiabetic activities of Tecoma stans (L.) Juss. ex Kunth. *J. Ethnopharmacol.* **2009**, *124*, 284–288, https://doi.org/10.1016/j.jep.2009.04.033.
12. Shin, S.; Soe, K.T.; Lee, H.; Kim, T.H.; Lee, S.; Park, M.S. A Systematic Map of Agroforestry Research Focusing on Ecosystem Services in the Asia-Pacific Region. *Forests* **2020**, *11*, 368, https://doi.org/10.3390/f11040368.
13. Anand, M.; Basavaraju, R. A review on phytochemistry and pharmacological uses of Tecoma stans (L.) Juss. ex Kunth. *J. Ethnopharmacol.* **2021**, *265*, 113270, https://doi.org/10.1016/j.jep.2020.113270.
14. Vijayaram, S.; Kannan, S.; Saravanan, K.M.; Vasantharaj, S.; Sathiyavimal, S.; P, P.S. Preliminary phytochemical screening, Antibacterial potential and GC-MS analysis of two medicinal plant extracts. *Pak. J. Pharm. Sci.* **2016**, *29*, 819–22.
15. Kumar, K.G.; Boopathi, T. An Updated overview on Pharmacognostical and Pharmacological Screening of Tecoma Stans. *Pharmatutor* **2018**, *6*, 38, https://doi.org/10.29161/PT.v6.i1.2018.38.
16. Meelah, M.M.; Mdee, L.K.; Eloff, J.N. *Tecoma stans* (Bignoniaceae), leaf extracts, fractions and isolated compound have promising activity against fungal phytopathogens. *Suid-Afrikaanse Tydskr. vir Natuurwetenskap en Tegnol.* **2017**, *36*, https://doi.org/10.4102/satnt.v36i1.1489.
17. Costantino, L.; Raimondi, L.; Pirisino, R.; Brunetti, T.; Pessotto, P.; Giannessi, F.; Lins, A.P.; Barlocco, D.; Antolini, L.; El-Abady, S.A. Isolation and pharmacological activities of the Tecoma stans alkaloids. *Farm.* **2003**, *58*, 781–785, https://doi.org/10.1016/S0014-827X(03)00133-2.
18. Ittagi, S.; Merugumolu, V.K.; Siddamsetty, R.S. Cardioprotective effect of hydroalcoholic extract of Tecoma stans flowers against isoproterenol induced myocardial infarction in rats. *Asian Pacific J. Trop. Dis.* **2014**, *4*, S378–S384, https://doi.org/10.1016/S2222-1808(14)60474-6.
19. Madire, L.G.; Netshiluvhi, M. Recent Advances in the Biological Control of *Tecoma stans* L. (Bignoniaceae) in South Africa. *African Entomol.* **2021**, *29*, 889–895, https://doi.org/10.4001/003.029.0889.
20. Weissig, V.; Elbayoumi, T.; Flühmann, B.; Barton, A. The Growing Field of Nanomedicine and Its Relevance to Pharmacy Curricula. *Am. J. Pharm. Educ.* **2021**, *85*, 8331, https://doi.org/10.5688/ajpe8331.
21. Fincheira, P.; Tortella, G.; Seabra, A.B.; Quiroz, A.; Diez, M.C.; Rubilar, O. Nanotechnology advances for sustainable agriculture: current knowledge and prospects in plant growth modulation and nutrition. *Planta* **2021**, *254*, 66, https://doi.org/10.1007/s00425-021-03714-0.
22. Ahmed, H.M.; Roy, A.; Wahab, M.; Ahmed, M.; Othman-Qadir, G.; Elesawy, B.H.; Khandaker, M.U.; Islam, M.N.; Emran, T.B. Applications of Nanomaterials in Agrifood and Pharmaceutical Industry. *J. Nanomater.* **2021**, *2021*, 1472096, https://doi.org/10.1155/2021/1472096.
23. Vromans, R.D.; van Eenbergen, M.C.; Geleijnse, G.; Pauws, S.; van de Poll-Franse, L. V; Krahmer, E.J. Exploring Cancer Survivor Needs and Preferences for Communicating Personalized Cancer Statistics From Registry Data: Qualitative Multimethod Study. *JMIR Cancer* **2021**, *7*, e25659, https://doi.org/10.2196/25659.
24. Govindan, P.; Manjusha, P.; Saravanan, K.M.; Natesan, V.; Salmen, S.H.; Alfarraj, S.; Wainwright, M.; Shakila, H. Expression and preliminary characterization of the potential vaccine candidate LipL32 of leptospirosis. *Appl. Nanosci.* **2021**, https://doi.org/10.1007/s13204-021-02097-8.
25. Shang, Y.; Zhang, X.; Lu, L.; Jiang, K.; Krohn, M.; Matschos, S.; Mullins, C.S.; Vollmar, B.; Zechner, D.; Gong, P.; *et al*. Pharmaceutical immunoglobulin G impairs anti-carcinoma activity of oxaliplatin in colon cancer cells. *Br. J. Cancer* **2021**, *124*, 1411–1420, https://doi.org/10.1038/s41416-021-01272-6.
26. Rajamurugan, R.; Thirunavukkarasu, D.C.; Sakthivel, V.; Sivashanmugam, M.; Raghavan, C.M. Phytochemical screening, antioxidant and antimicrobial activities of ethanolic extract of Tecoma Stans flowers. *Int. J. Pharma Bio Sci.* **2013**, *4*, P124–P130.
27. Anand, M. Phytochemical analysis of Tecomastans (L.) Juss ex Kunth leaves from Puttaparthi, Andhra Pradesh, India. *Int. J. Curr. Res.* **2016**, *8*, 34632–34635.
28. Prasad, R.; Swamy, V.S. Antibacterial Activity of Silver Nanoparticles Synthesized by Bark Extract of *Syzygium cumini*. *J. Nanoparticles* **2013**, *2013*, 431218, https://doi.org/10.1155/2013/431218.

29. Anand, A.V.; Bharathi, V.; Bupesh, G.; Lakshmi, N.J.; Sundaram, K.M.; Saradhadevi, K.M. Identification of novel potent pancreatic lipase inhibitors from ficus racemosa. *Biomed.* **2021**, *41*, 23–30, https://doi.org/10.51248/.v41i1.528.
30. Shaikh, S.; Nazam, N.; Rizvi, S.M.D.; Ahmad, K.; Baig, M.H.; Lee, E.J.; Choi, I. Mechanistic Insights into the Antimicrobial Actions of Metallic Nanoparticles and Their Implications for Multidrug Resistance. *Int. J. Mol. Sci.* **2019**, *20*, 2468, https://doi.org/10.3390/ijms20102468.
31. Ha, K.-N.; Nguyen, T.-V.-A.; Mai, D.-T.; Tran, N.-M.-A.; Nguyen, N.-H.; Vo, G. Van; Duong, T.-H.; Truong Nguyen, H. Alpha-glucosidase inhibitors from Nervilia concolor, Tecoma stans, and Bouea macrophylla. *Saudi J. Biol. Sci.* **2022**, *29*, 1029–1042, https://doi.org/10.1016/j.sjbs.2021.09.070.

Supplementary materials

Supplementary Table 1. The phytochemical screening of natural compounds. ++ indicates present in more quantity of the phytoconstituents. + Indicates the presence of phytoconstituents.

Plant constituents	Result	Inference
Alkaloids	+	White or yellow precipitate
Steroids	++	Red violet color
Terpenoids	++	Golden yellow color
Flavonoids	++	Colourless
Saponins	++	Foam formation
Phenols	+	Formation of color
Glycosides	++	Yellow color
Tannins	++	Bluish black color

Supplementary Table 2. FTIR study of *T. stans* leaf extracts (crude and AgNPs). Represents the presence of various functional compounds in both the crude and AgNP synthesized leaf extracts of *T. stans*.

Class of compounds	Absorption, cm^{-1} of *T. stans* crude leaf extracts	Absorption, cm^{-1} of *T. stans* leaf AgNPs
Alkanes and alkyls	2852.16, 1383.45	2854.58,2923.81,1383.74
Alkenes	667.87	668.20
Alkyl halides	667.87, 1019.50	1089.31,1270.70,1319.29,779.91, 558.15, 602.81, 668.20,418.93,480.35
Alcohols	3399.88	1089.31
Ethers	-	1270.70
Aldehydes	-	1626.01
ketones	1743.38	1741.96
Carboxylic acids	-	2854.58,2923.91,3420.81
Esters	1743.38	1270.70
Amides	3399.88	1626.02
Aromatic compounds	-	779.91

Supplementary Table 3. FTIR study of *T. stans* leaf extracts (crude and AgNPs). Represents various functional compounds present in both the crude and AgNPs synthesized using flower extracts of *T. stans*.

Class of compounds	Absorption, cm^{-1} of *T. stans* crude flower extracts	Absorption, cm^{-1} of *T. stans* flower AgNPs
Alkyl halides	417.74,462.10,489.64,554.31, 1054.19,1270.81,1318.82	408.23,437.06,466.81,600.92, 667.15,1024.96,1271.78,1319.94
Alkanes, alkyls	1383.53	1383.56,1458.84,2854.80, 2924.29
Amides	1622.08,3416.71	1634.77,3425.55
Carboxylic acids	2854.73,2924.47	-
Ketones	1742.45	1742.19
Alkenes	-	874.57

Supplementary Table 4. A represents zone of inhibition of *T. stans* leaf and B. represents zone of inhibition of *T. stans* flower.

A

Microorganism	Zone of inhibition in mm			
	10µg	20µg	30µg	40µg
E.Coli	8	10	15	18
K.Pnuemonia	5	10	12	16
S.Aureus	-	8	6	10
B.subtilis	-	5	6	8

B

Microorganism	**Zone of inhibition(mm)**			
	10µg	**20µg**	**30µg**	**40µg**
E.coli	-	6	10	12
B.subtilis	8	10	12	14
S.aureus	12	14	16	18
K.penumonia	-	8	10	12

Supplementary Table 5. Mentions the percentage of anti-oxidant activity of *T. stans* leaf (A) and flower (B).

A

Concentration (µg/ml)	Crude (% of absorption)	AgNPs (% of absorption)
100	19.49	21.812
200	29.86	35.923
300	40.668	43.76
400	57.66	60.438
500	66.57	70.694

B

Concentration	% of absorption of crude	% of absorption of AgNPs
100µg/ml	18%	23%
200 µg/ml	41%	47%
300 µg/ml	55%	58%
400 µg/ml	66%	70%
500 µg/ml	76%	81%

Supplementary Figure S1. A-F represents the anti-proliferative activity against the *T. stans* AgNP flower extracts at different concentrations.

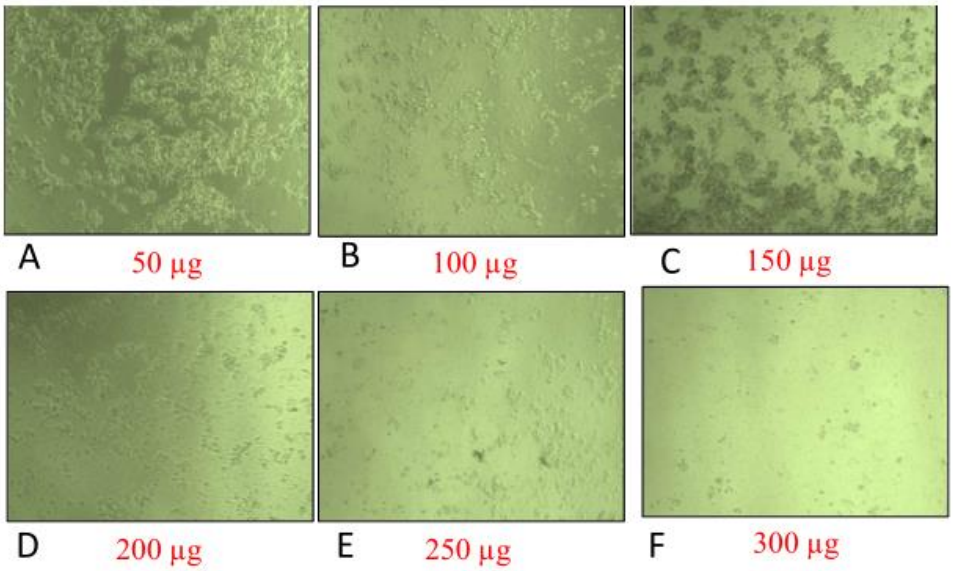

Supplementary Figure S2. Represents the graphical representation of anti-proliferative activity against colorectal cancer cell lines. HEK 293 is used as a control.

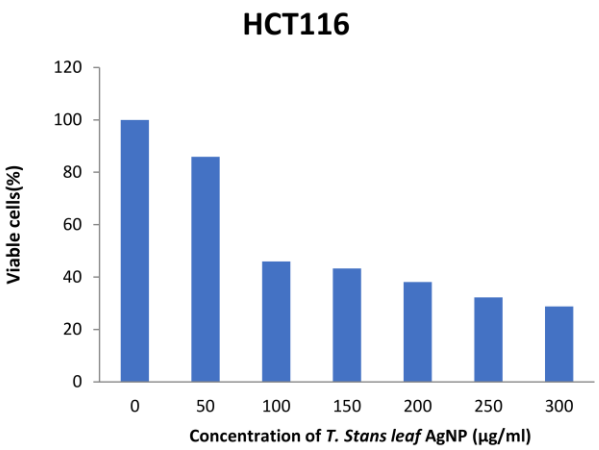
HCT116
Viable cells(%)
120
100
80
60
40
20
0
0
50
100
150
200
250
300
Concentration of T. Stans leaf AgNP (µg/ml)

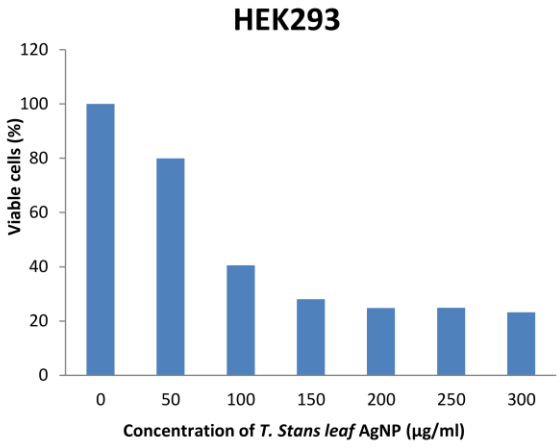
HEK293
Viable cells (%)
120
100
80
60
40
20
0
0
50
100
150
200
250
300
Concentration of T. Stans leaf AgNP (µg/ml)

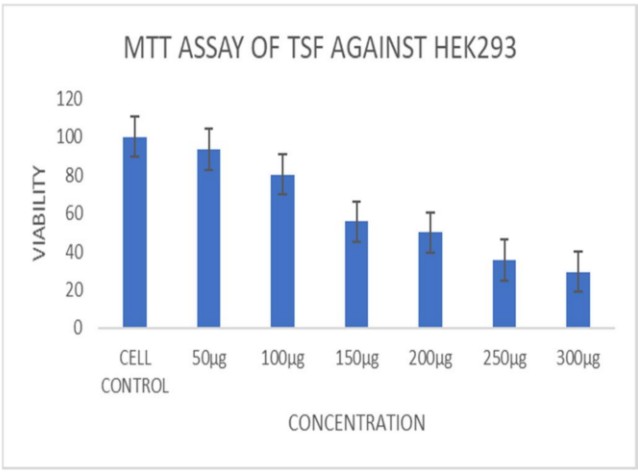
MTT ASSAY OF TSF AGAINST HEK293
VIABILITY
120
100
80
60
40
20
0
CELL CONTROL
50µg
100µg
150µg
200µg
250µg
300µg
CONCENTRATION

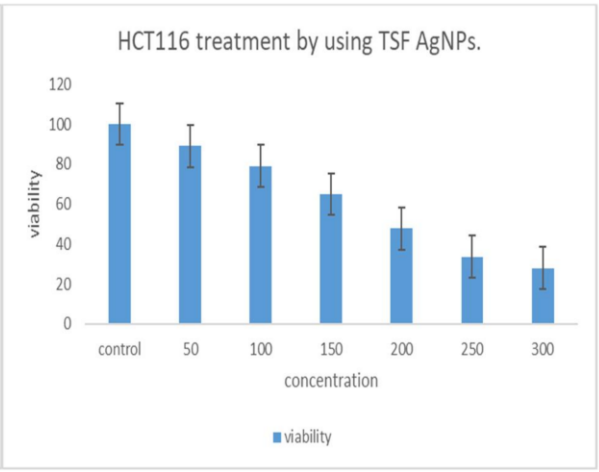
HCT116 treatment by using TSF AgNPs.
viability
120
100
80
60
40
20
0
control
50
100
150
200
250
300
concentration
viability